

LETTER • OPEN ACCESS

Significant climate benefits from near-term climate forcer mitigation in spite of aerosol reductions

To cite this article: Robert J Allen *et al* 2021 *Environ. Res. Lett.* **16** 034010

View the [article online](#) for updates and enhancements.

You may also like

- [Autoregressive Planet Search: Application to the *Kepler* Mission](#)
Gabriel A. Caceres, Eric D. Feigelson, G. Jogesh Babu *et al.*
- [Structure of the simple harmonic-repulsive system in liquid and glassy states studied by the triple correlation function](#)
V A Levashov, R E Ryltsev and N M Chchelkatchev
- [Optical, thermal and electrical properties of pure and doped bis-thiourea cadmium formate \(BTCF\) crystal](#)
N N Shejwal, Mohd Anis, S S Hussaini *et al.*

ENVIRONMENTAL RESEARCH
LETTERS

LETTER

Significant climate benefits from near-term climate forcer mitigation in spite of aerosol reductions

OPEN ACCESS

RECEIVED

26 September 2020

REVISED

13 December 2020

ACCEPTED FOR PUBLICATION

27 January 2021

PUBLISHED

15 February 2021

Original Content from this work may be used under the terms of the [Creative Commons Attribution 4.0 licence](#).

Any further distribution of this work must maintain attribution to the author(s) and the title of the work, journal citation and DOI.



Robert J Allen¹ , Larry W Horowitz², Vaishali Naik², Naga Oshima³ , Fiona M O'Connor⁴, Steven Turnock⁴, Sungbo Shim⁵, Philippe Le Sager⁶, Twan van Noije⁶, Kostas Tsigaridis⁷, Susanne E Bauer⁷, Lori T Sentman², Jasmin G John², Conor Broderick^{2,8}, Makoto Deushi³ , Gerd A Folberth⁴, Shinichiro Fujimori^{9,10,11} and William J Collins¹²

- ¹ University of California Riverside, Department of Earth and Planetary Sciences, Riverside, CA, United States of America
- ² DOC/NOAA/OAR/Geophysical Fluid Dynamics Laboratory, Biogeochemistry, Atmospheric Chemistry, and Ecology Division, Princeton, NJ, United States of America
- ³ Meteorological Research Institute, Japan Meteorological Agency, Tsukuba, Ibaraki, Japan
- ⁴ Met Office Hadley Centre, Exeter, United Kingdom
- ⁵ National Institute of Meteorological Sciences, Seogwipo-si, Jeju-do, Republic of Korea
- ⁶ Royal Netherlands Meteorological Institute (KNMI), De Bilt, The Netherlands
- ⁷ Center for Climate Systems Research, Columbia University, NASA Goddard Institute for Space Studies, New York, NY, United States of America
- ⁸ Macalester College, St. Paul, MN, United States of America
- ⁹ Department of Environmental Engineering, Kyoto University, C1-3 361, Kyotodaigaku Katsura, Nishikyoku, Kyoto, Japan
- ¹⁰ Center for Social and Environmental Systems Research, National Institute for Environmental Studies (NIES), 16-2 Onogawa, Tsukuba, Ibaraki, Japan
- ¹¹ International Institute for Applied System Analysis (IIASA), Schlossplatz 1, Laxenburg, Austria
- ¹² Department of Meteorology, University of Reading, Reading, United Kingdom

E-mail: rjallen@ucr.edu

Keywords: NTCF, SLCF, aerosol, ozone, methane, mitigation

Supplementary material for this article is available [online](#)

Abstract

Near-term climate forcers (NTCFs), including aerosols and chemically reactive gases such as tropospheric ozone and methane, offer a potential way to mitigate climate change and improve air quality—so called ‘win-win’ mitigation policies. Prior studies support improved air quality under NTCF mitigation, but with conflicting climate impacts that range from a significant reduction in the rate of global warming to only a modest impact. Here, we use state-of-the-art chemistry-climate model simulations conducted as part of the Aerosol and Chemistry Model Intercomparison Project (AerChemMIP) to quantify the 21st-century impact of NTCF reductions, using a realistic future emission scenario with a consistent air quality policy. Non-methane NTCF (NMNTCF; aerosols and ozone precursors) mitigation improves air quality, but leads to significant increases in global mean precipitation of 1.3% by mid-century and 1.4% by end-of-the-century, and corresponding surface warming of 0.23 and 0.21 K. NTCF (all-NTCF; including methane) mitigation further improves air quality, with larger reductions of up to 45% for ozone pollution, while offsetting half of the wetting by mid-century (0.7% increase) and all the wetting by end-of-the-century (non-significant 0.1% increase) and leading to surface cooling of -0.15 K by mid-century and -0.50 K by end-of-the-century. This suggests that methane mitigation offsets warming induced from reductions in NMNTCFs, while also leading to net improvements in air quality.

1. Introduction

Near-term climate forcers (NTCFs), also known as short-lived climate forcers (SLCFs), include aerosols such as sulfate, nitrate, organic carbon (OC) and black carbon (BC) and chemically reactive gases

including ozone (O_3), sulfur dioxide and methane (CH_4). Although often co-emitted with long-lived greenhouse gases (GHGs) including carbon dioxide (CO_2), the impact of NTCFs largely occurs within the first decade after their emission (Myhre *et al* 2013). NTCF mitigation has received considerable attention,

as aerosols and ozone are sources of air pollution (Fiore *et al* 2012), which is associated with adverse human health and ecosystem impacts (WHO 2016, Butt *et al* 2017, Cohen *et al* 2017). NTCFs also affect the radiative balance of the Earth, leading to a climate forcing nearly equal in magnitude to that of CO₂ (Myhre *et al* 2013, Shindell *et al* 2013). This forcing drives climate perturbations, including surface warming (CH₄, BC, some OC components, O₃) or cooling (sulfate, nitrate, OC), as well as altered precipitation patterns (Allen 2015, Allen *et al* 2015, Rotstajn *et al* 2015b, Liu *et al* 2018). In the context of methane forcing, recent studies show the importance of shortwave absorption, which increases the radiative forcing by ~20%–25% and also acts to mute precipitation increases due to fast adjustment processes associated with enhanced atmospheric stability (Collins *et al* 2006, Etmann *et al* 2016, Modak *et al* 2018). NTCF mitigation is therefore of particular importance to both the United Nation's Sustainable Development Goals (Haines *et al* 2017, Lelieveld 2017, Shindell *et al* 2017), as well as the Paris Agreement, which strives to keep global mean surface temperature to well below 2 °C above preindustrial values (IPCC 2018). Policies that combine both climate and air pollution mitigation ('win-win' policies) have clear societal and economic benefits compared to separate mitigation (Clarke *et al* 2014). It is thus of interest to evaluate NTCF mitigation.

Many studies have addressed the impact of NTCF mitigation on air quality and climate. Although air quality is improved in response to rapid removal of anthropogenic aerosols, large near-term increases in surface temperature and precipitation also occur (Andreae *et al* 2005, Brasseur and Roeckner 2005, Ramanathan and Feng 2008, Arneth *et al* 2009, Raes and Seinfeld 2009, Kloster *et al* 2010, Matthews and Zickfeld 2012, Rotstajn *et al* 2013, Wu *et al* 2013, Westervelt *et al* 2015, Salzmann 2016, Hienola *et al* 2018, Richardson *et al* 2018, Samset *et al* 2018). The importance of reducing methane emissions to simultaneously mitigate climate change and improve air quality was first highlighted by Shindell *et al* (2012). Since then, a few studies have explored air quality and climate change benefits from concomitant decline in methane, aerosols and ozone precursors (UNEP 2011, Smith and Mizrahi 2013, Stohl *et al* 2015, Jones *et al* 2018, Lelieveld *et al* 2019, Shindell and Smith 2019, Turnock *et al* 2019) employing either idealized scenarios or simple reduced-complexity climate models. Although these studies show improved air quality under NTCF mitigation, they yield conflicting climate impacts that range from a significant reduction in the rate of global warming to only a modest impact. For example, Smith and Mizrahi (2013) show that with maximally feasible BC and CH₄ reductions phased in from 2015 to 2035, global mean temperatures in 2050 would be reduced by only 0.16 K (uncertainty range of 0.04–0.35 K) relative to

a reference scenario with no explicit GHG policies, with more realistic emission reductions likely providing an even smaller climate benefit. In contrast, Stohl *et al* (2015) show that reducing CH₄ and BC emission by 50% and 80%, respectively, relative to current legislation will reduce warming by 0.22 ± 0.07 by 2041–2050, with the largest warming reduction of 0.44 (0.39–0.49) K over the Arctic. Similarly, UNEP (2011) shows that CH₄, BC and O₃ mitigation will reduce global warming by 0.4 (0.1–0.6) K by 2050, effectively halving the rate of projected warming.

In terms of hydrological impacts, most NTCF mitigation studies have focused on the impacts of aerosols alone. Samset *et al* (2018) show that complete removal of present-day anthropogenic aerosol emissions induces a global mean precipitation increase of 2%–4.6%. Future aerosol reductions may also shift the tropical rainbelt northward, and strengthen precipitation in several monsoon regions, including West Africa, South Asia, and East Asia (Levy *et al* 2013, Allen 2015, Rotstajn *et al* 2015a, Allen and Ajoku 2016, Westervelt *et al* 2017, Westervelt *et al* 2018, Zhao *et al* 2018, Scannell *et al* 2019, Zanis *et al* 2020). Lelieveld *et al* (2019) find precipitation increases of 10%–70% over India, 10%–30% over northern China, and 10%–40% over Central America, West Africa, and the Sahel in response to removal of anthropogenic emissions, largely due to aerosol emissions reductions. Stohl *et al* (2015) find that CH₄ and BC mitigation increases precipitation (~4%) from spring to autumn in the Mediterranean region, which would help alleviate the expected future water shortages in this region.

Allen *et al* (2020) recently analyzed simulations from the the Aerosol and Chemistry Model Intercomparison Project (AerChemMIP) (Collins *et al* 2017), part of the Coupled Model Intercomparison Project (CMIP6) (Eyring *et al* 2016), with models that include an interactive representation of tropospheric aerosols and atmospheric chemistry, allowing for the quantification of chemistry-climate interactions. They found that relative to the Shared Socioeconomic Pathway 3-7.0 (SSP3-7.0; with strong increases in GHGs and NTCFs), NMNTCF (aerosols and ozone precursors) mitigation in the SSP3-7.0-lowNTCF scenario leads to mid-21st century (2015–2055) surface temperature and precipitation increases of 0.25 ± 0.12 K and 0.03 ± 0.012 mm d⁻¹, respectively, as well as increases in extreme weather indices, including the hottest and wettest day. Larger warming and wetting occurred over some regions, particularly Asia, as well as in the Arctic. Moreover, these responses were largely due to the decrease in aerosols, as opposed to ozone precursors. This study, however, extended only to mid-21st century and did not address the impacts of methane reductions. It remains unclear if methane mitigation can prevent the warming that results from reductions in NMNTCFs, as well as the impact of methane mitigation on air quality.

Here, we extend the results of Allen *et al* (2020) using NMNTCF simulations that now extend through the 21st-century and new AerChemMIP 21st century NTCF simulations that include methane (as well as aerosol and ozone precursors) reductions, focused on the surface temperature, precipitation and air quality impacts due to NTCF mitigation. Consistent with prior work, we show that NMNTCF reductions improve air quality, but also lead to additional surface warming and wetting throughout the 21st century. NTCF reductions that include methane (all-NTCF), however, compensate for this warming in the short term (mid-century) and more than offset this warming in the long term (end of century). Much of the NMNTCF precipitation increase is also offset by the end of the century under all-NTCF mitigation. All-NTCF mitigation also leads to additional improvements in air quality, particularly in terms of ozone. This paper is organized as follows: Methods are presented in section 2 and results are discussed in section 3. Conclusions appear in section 4.

2. Methods

2.1. Future Emission Scenarios

As part of ScenarioMIP, a set of SSPs (O'Neill *et al* 2014, van Vuuren *et al* 2014, Eyring *et al* 2016, Gidden *et al* 2019) have been developed for CMIP6. To detect the impact of air quality pollutants, AerChemMIP uses SSP3-7.0 ($\sim 7.0 \text{ W m}^{-2}$ at 2100) as the reference scenario, which lacks climate policy, has 'weak' levels of air quality control measures and thus the highest levels of NTCFs (O'Neill *et al* 2014, Fujimori *et al* 2017, Rao *et al* 2017). To isolate the effects of air quality controls, the SSP3-7.0-lowNTCF scenario (Gidden *et al* 2019) was developed, using the same socio-economic scenario and the same emissions drivers (e.g. population, GDP, energy and land-use), but with 'strong' levels of air quality control measures. In the case of air pollutant species (e.g. sulfur, BC, OC, NO_x), the emissions factors assumed in SSP1—a sustainability pathway—are adopted. Here, the decrease in air pollutant species emissions is due to swift ramping up of end-of-pipe measures for air pollution control (rather than a transition to non-fossil-based fuels). This assumption implicitly assumes that SSP1's air pollutant legislation and technological progress can be achieved in the SSP3 world. Thus, the decrease in air pollutant species emissions is due to the aggressive air pollution policy alone. In the case of CH₄, the CH₄ emissions' reduction rates in SSP1-2.6 relative to the SSP1 baseline are adopted to SSP3-7.0. This implicitly assumes that SSP3-7.0-lowNTCF can reduce CH₄ as if SSP1's stringent climate mitigation policy is implemented in the SSP3 world. We acknowledge that the lowNTCF pathway is unlikely to occur in reality, and that our results (e.g. the magnitude of the surface temperature

increase) likely represent an upper bound as the baseline scenario (SSP3-7.0) contains the highest levels of NTCFs.

In addition to the SSP3-7.0 reference experiment, which is part of the Scenario Model Inter-comparison Project (ScenarioMIP) (O'Neill *et al* 2016), two sets of experiments were run based on the SSP3-7.0-lowNTCF scenario. The first low NTCF experiment, SSP3-7.0-lowNTCF (Collins *et al* 2017, Allen *et al* 2020), excludes the methane changes. An additional experiment—SSP3-7.0-lowNTCFCH₄—was therefore run that includes both methane and NMNTCFs. Thus, the SSP3-7.0-lowNTCF experiment, which we henceforth refer to as strong non-methane air quality control, allows quantification of the climate and air quality impacts due to NMNTCFs (supplementary table 1 (available online at stacks.iop.org/ERL/16/034010/mmedia)). The SSP3-7.0-lowNTCFCH₄ experiment, which we henceforth refer to as strong air quality control, allows the impacts of all NTCFs (including methane) to be quantified. Furthermore, we define NMNTCF mitigation as the difference between the strong non-methane air quality control experiment and the weak air quality control experiment (SSP3-7.0-lowNTCF—SSP3-7.0; supplementary table 1). Similarly, all-NTCF mitigation is defined as the difference between the strong and weak air quality control experiment (SSP3-7.0-lowNTCFCH₄—SSP3-7.0). Finally, methane mitigation alone is defined as the difference between the two strong air quality control experiments (with and without methane reductions, SSP3-7.0-lowNTCFCH₄—SSP3-7.0-lowNTCF).

Under weak air quality control (supplementary figure 1), global mean atmospheric CO₂ and CH₄ concentrations (models are concentration-driven for these species) increase by $\sim 35\%$ by mid-century, with continued increases of 116% and 83%, respectively, by 2100 (relative to 2015). Global emissions of all aerosols and gaseous precursors (models are emission-driven for these species) also increase by 7%–13% by mid-century (except SO₂), but then decrease afterwards due to end-of-pipe measures for air pollution control. By 2100, most of these species have decreased relative to 2015, ranging from ~ 0 (for volatile organic compounds, VOCs) to -22% (for SO₂). In contrast, strong air quality control yields emission reductions in all aerosol and gaseous precursors, particularly during the first half of the century, ranging from -26% for VOCs to -54% for SO₂. This decrease under strong air quality control continues (although more weakly) through 2100, with aerosol and gaseous precursor emissions decreasing by -52% to -68% . Similarly, CH₄ concentrations decrease by -26% and -34% by mid-century and end-of-the-century, respectively (CO₂ concentrations are identical to those under weak air quality control).

Table 1. Climate and air pollution changes under NMNTCF, all-NTCF and methane mitigation. Global annual mean changes in surface temperature (T_s), precipitation (Precip), surface ozone (O_3), surface particulate matter ($PM_{2.5}$) and the effective radiative forcing (ERF) for (top) NMNTCF, (middle) all-NTCF and (bottom) methane mitigation. First (second) set of numbers is the 2050–2059 (2090–2099) change relative to 2005–2014. Changes not significant at the 95% confidence level based on a t -test are denoted by bold font. Units are K for T_s ; $mm\ d^{-1}$ for Precip; ppb for O_3 ; $\mu g\ m^{-3}$ for $PM_{2.5}$; and $W\ m^{-2}$ for ERF. MMM (last rows) is the multi-model mean.

	NMNTCF mitigation				
	T_s	Precip	O_3	$PM_{2.5}$	ERF
GFDL-ESM4	0.15/ 0.06	0.033/0.038	−4.46/−4.76	−0.80/−0.78	0.020/0.17
UKESM1-0-LL	0.24/0.26	0.041/0.044	−3.15/−3.59	−0.90/−0.87	0.36/0.35
MRI-ESM2-0	0.19/0.29	0.040/0.049	−4.38/−4.92	−1.04/−0.98	0.45/0.66
EC-Earth3-AerChem	0.45/0.46	0.066/0.067	−5.43/−5.66	−0.89/−0.94	0.64/0.68
GISS-E2-1-G	0.15/− 0.02	0.019/0.010	−6.10/−6.01	−0.58/−0.52	0.37/0.35
MMM	0.23/0.21	0.040/0.041	−4.70/−4.99	−0.84/−0.82	0.37/0.44
	All-NTCF mitigation				
	T_s	Precip	O_3	$PM_{2.5}$	ERF
GFDL-ESM4	−0.10/−0.41	0.035/0.027	−7.47/−8.85	−0.91/−1.07	−0.61/−1.05
UKESM1-0-LL	−0.34/−0.88	0.006 /−0.030	−6.21/−7.54	−0.91/−0.89	−0.62/−1.14
MRI-ESM2-0	−0.12/−0.34	0.024/0.014	−7.30/−9.26	−1.01/−1.02	−0.31/−0.61
EC-Earth3-AerChem	− 0.01 /−0.50	0.034/ 0.006	−9.06/−11.18	−0.99/−1.04	−0.20/−0.70
GISS-E2-1-G	−0.19/−0.40	0.009/0.004	−7.73/−8.36	−0.61/−0.61	−0.39/−0.64
MMM	−0.15/−0.50	0.022/ 0.004	−7.56/−9.04	−0.88/−0.93	−0.42/−0.83
	Methane mitigation				
	T_s	Precip	O_3	$PM_{2.5}$	ERF
GFDL-ESM4	−0.26/−0.47	0.001 /−0.010	−3.01/−4.10	−0.11/−0.29	−0.63/−1.22
UKESM1-0-LL	−0.57/−1.14	−0.036/−0.074	−3.07/−3.95	− 0.01 /− 0.02	−0.98/−1.49
MRI-ESM2-0	−0.31/−0.63	−0.016/−0.035	−2.92/−4.34	0.03 /− 0.04	−0.76/−1.27
EC-Earth3-AerChem	−0.46/−0.96	−0.031/−0.062	−3.63/−5.52	− 0.09 /− 0.11	−0.84/−1.38
GISS-E2-1-G	−0.34/−0.38	− 0.010 /−0.006	−1.63/−2.34	− 0.03 /−0.09	−0.75/−1.00
MMM	−0.39/−0.71	−0.018/−0.037	−2.85/−4.05	− 0.04 /−0.11	−0.79/−1.27

2.2. AerChemMIP models

Five coupled ocean-atmosphere-chemistry climate models performed the necessary simulations, including GFDL-ESM4 (Horowitz *et al* 2018, John *et al* 2018, Dunne *et al* 2020, Horowitz *et al* 2020), UKESM1-0-LL (Sellar *et al* 2019, Archibald *et al* 2020, Mulcahy *et al* 2020), MRI-ESM2-0 (Yukimoto *et al* 2019, Oshima *et al* 2020), EC-Earth3-AerChem (van Noije *et al* 2014, van Noije *et al* 2020) and GISS-E2-1-G (Bauer *et al* 2020). All models performed at least one 2015–2100 realization for each of the three experiments described above, with UKESM1-0-LL, MRI-ESM2-0 and GISS-E2-1-G performing three realizations of each. Each model also performed similar experiments with fixed sea surface temperatures (SSTs) to estimate the effective radiative forcing (ERF). The three coupled experiments are repeated with prescribed SSTs and sea ice, taken from the monthly mean evolving values from the base SSP3-7.0 coupled simulation (Collins *et al* 2017). All analyses are based on archived monthly mean data, which is subsequently averaged to obtain annual means, and all data is spatially interpolated to a $2.5^\circ \times 2.5^\circ$ grid using bilinear interpolation. The

multi-model mean (MMM) is obtained by averaging each model's mean response (i.e. each model has the same weight). We reiterate that these models are driven by GHG (e.g. CO_2 , CH_4) concentrations, as opposed to emissions.

2.3. Methodology

Changes in surface temperature, precipitation, ERF and air quality—including both surface ozone (O_3) and particulate matter less than $2.5\ \mu m$ in diameter ($PM_{2.5}$)—are estimated by taking a difference of means, focused on two time periods: mid-century (2050–2059 relative to 2005–2014), as well as end-of-the-century (2090–2099 relative to 2005–2014). Data for 2005–2014 comes from the model's corresponding historical simulations. Due to lack of a historical SST experiment, ERF changes for EC-Earth3-AerChem are relative to 2015. Furthermore, we only evaluate ERF changes under mitigation (difference of experiments); it is not possible to get an ERF response in the default simulations since SSTs change between 2005–2014 and 2050–2059/2090–2099. Significance is based on a standard t -test for the difference of means, where $t = \frac{\bar{x}_1 - \bar{x}_2}{SE}$, where \bar{x}_1 and \bar{x}_2 are means

during two periods (e.g. 2050–2059 and 2005–2014) and SE is the standard error, which is estimated as $\sqrt{\frac{s_1^2}{n_1} + \frac{s_2^2}{n_2}}$. Here, n_1 and n_2 are the number of years in time period 1 and 2, and s_1 and s_2 are the corresponding standard deviations. The degrees of freedom are estimated as: $\frac{(s_1^2/n_1 + s_2^2/n_2)^2}{(s_1^2/n_1)^2/(n_1-1) + (s_2^2/n_2)^2/(n_2-1)}$.

The ERF is calculated from the top-of-the-atmosphere (TOA) radiative flux differences between atmosphere-only simulations with identical SSTs but differing composition (Forster *et al* 2016, Pincus *et al* 2016). Although this is not strictly an ERF, because the climate (specifically, land temperature) is changing, looking at the ERF differences between experiments is a feasible approach because the SSTs match. For ozone and PM_{2.5}, monthly mean fields are obtained from the model level closest to the surface. Since models include different aerosol species (e.g. nitrate and ammonium aerosol are only included in GFDL-ESM4, EC-Earth3-AerChem and GISS-E2-1-G) and not all models directly archive PM_{2.5}, and those that do use different methodologies (Allen *et al* 2020), we approximate PM_{2.5} using: $PM_{2.5} = BC + OA + SO_4 + 0.1 \times DU + 0.25 \times SS$, where BC is black carbon, OA is organic aerosol, SO₄ is sulfate aerosol, DU is dust and SS is sea salt (Fiore *et al* 2012, Silva *et al* 2017, Allen *et al* 2020). The ‘true’ DU and SS factors will be dependent on the model and its size distribution, but here we use 0.1 and 0.25, respectively. Although this PM_{2.5} approximation method introduces some uncertainty, it allows for not only an estimate of PM_{2.5} in all models, but a uniform estimate as well. CMIP6 model evaluation of air quality metrics, including surface O₃ and PM_{2.5} is quantified in a companion paper (Turnock *et al* 2020). To summarize, CMIP6 models generally underestimate PM_{2.5} over most regions relative to observations (possibly due to lack of nitrate aerosol in many models), whereas models consistently overestimate surface ozone across most regions during both summer and winter (potentially due to their coarse resolution).

3. Results

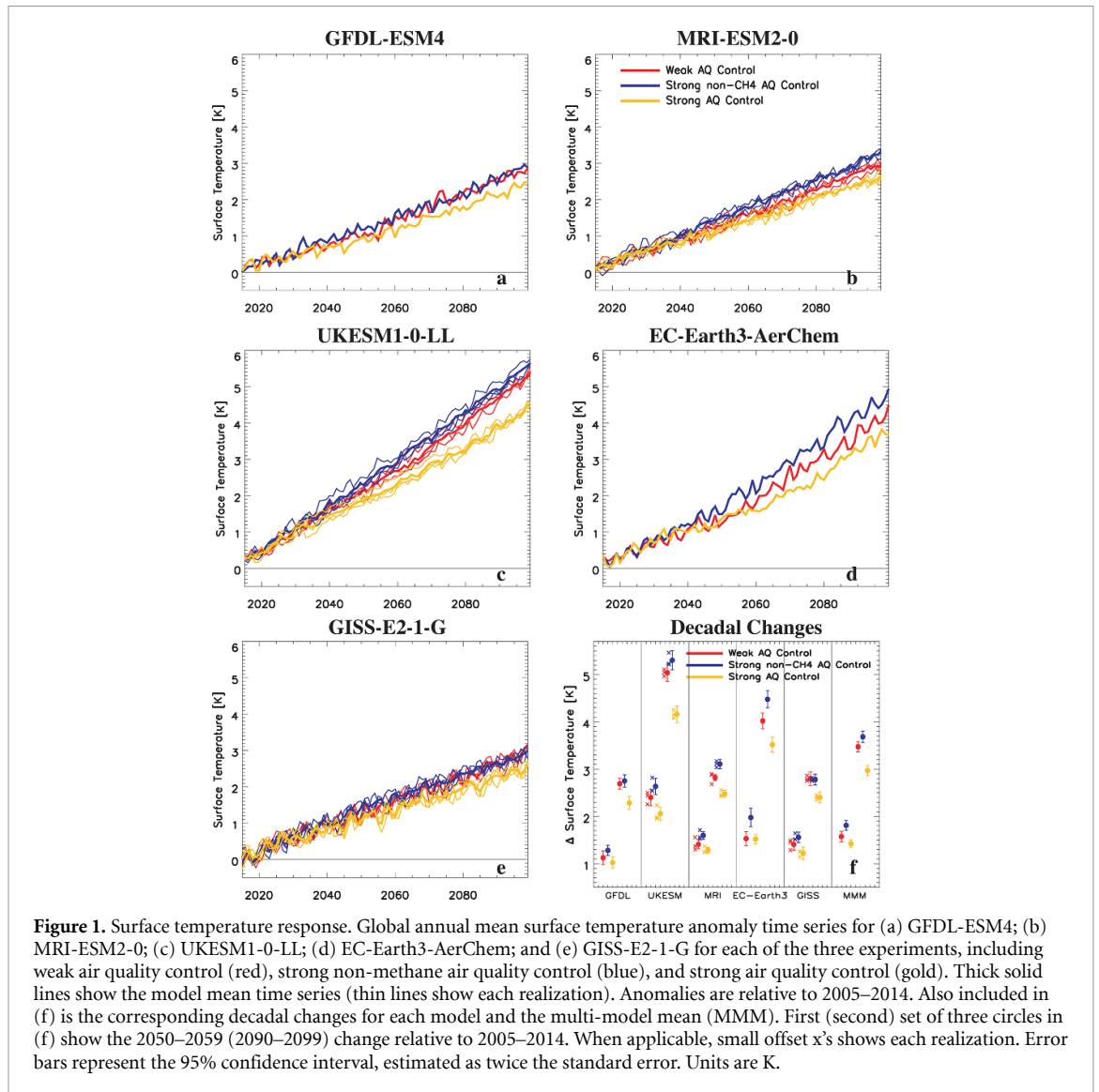
3.1. Surface temperature

Figure 1 shows each model’s global annual mean surface temperature anomaly times series for each of the three experiments (figures 1(a)–(e)), as well as the decadal changes in 2050–2059 and 2090–2099, relative to 2005–2014 (figure 1(f)). Weak air quality control yields significant increases in surface temperature for all models (but with relatively large inter-model spread), ranging from 1.12 to 2.40 K by mid-century and 2.69 to 5.04 K by end-of-the-century (figure 1(f)). GFDL-ESM4 yields the weakest increase, and UKESM1-0-LL yields the strongest increase—especially by 2100. The corresponding

MMM warming (figure 1(f) and see also supplementary figures 2–3) is 1.57 ± 0.11 by mid-century and 3.47 ± 0.11 K by end-of-the-century (uncertainty here and elsewhere is estimated as twice the standard error). Similar to Allen *et al* (2020), under strong non-methane air quality control, models show enhanced warming, again due to the decrease in aerosols and non-methane precursor gases that form aerosols and ozone (and similar GHG increases). Warming ranges from 1.28 to 2.63 K by mid-century and 2.75 to 5.30 K by end-of-the-century, with GFDL-ESM4 (UKESM1-0-LL) again yielding the smallest (largest) warming (figure 1(f)). The corresponding MMM warming is 1.81 ± 0.10 and 3.68 ± 0.12 K, respectively.

Consistent with the larger warming under strong non-methane air quality control, relative to weak air quality control, NMNTCF mitigation (figure 2(b) and table 1) yields net warming in nearly all models, ranging from 0.15 to 0.45 K by mid-century and -0.02 to 0.46 K by end-of-the-century, with MMM warming of 0.23 ± 0.05 and 0.21 ± 0.03 K, respectively. GFDL-ESM4 and GISS-E2-1-G yield the weakest warming (with GISS-E2-1-G yielding weak, non-significant cooling by end-of-the-century), implying the change in aerosol and ozone forcing is well-balanced in these models. In contrast, EC-Earth3-AerChem yields the largest warming under NMNTCF mitigation (figure 2(a) and table 1), implying larger aerosol—as opposed to ozone—forcing in this model. Significant warming under NMNTCF mitigation is in agreement with prior studies (Andreae *et al* 2005, Brasseur and Roeckner 2005, Ramanathan and Feng 2008, Arneth *et al* 2009, Raes and Seinfeld 2009, Kloster *et al* 2010, Matthews and Zickfeld 2012, Rotstayn *et al* 2013, Wu *et al* 2013, Westervelt *et al* 2015, Salzmann 2016, Hienola *et al* 2018, Richardson *et al* 2018, Samset *et al* 2018) and implies that reducing aerosols and non-methane precursor gases will accelerate global warming, particularly by mid-century when the bulk of the emissions reductions occur.

Compared to strong non-methane air quality control, strong air quality control (i.e. including methane) yields less warming during both time periods (figure 1(f)), ranging from 1.02 to 2.06 K by mid-century and 2.29 to 4.16 K by end-of-the-century, with corresponding MMM warming of 1.42 ± 0.08 and 2.96 ± 0.11 K. In fact, all-NCTF mitigation (figure 2(b) and table 1) yields significant global cooling in all cases except EC-Earth3-AerChem by mid-century, with MMM changes of -0.15 ± 0.05 by mid-century and -0.50 ± 0.02 K by end-of-the-century. This implies that methane emission reductions more than offset the aerosol and non-methane precursor gas-induced surface warming for both time periods. Methane mitigation yields strong MMM surface cooling at -0.39 ± 0.05 by mid-century and -0.71 ± 0.02 K by end-of-the-century.

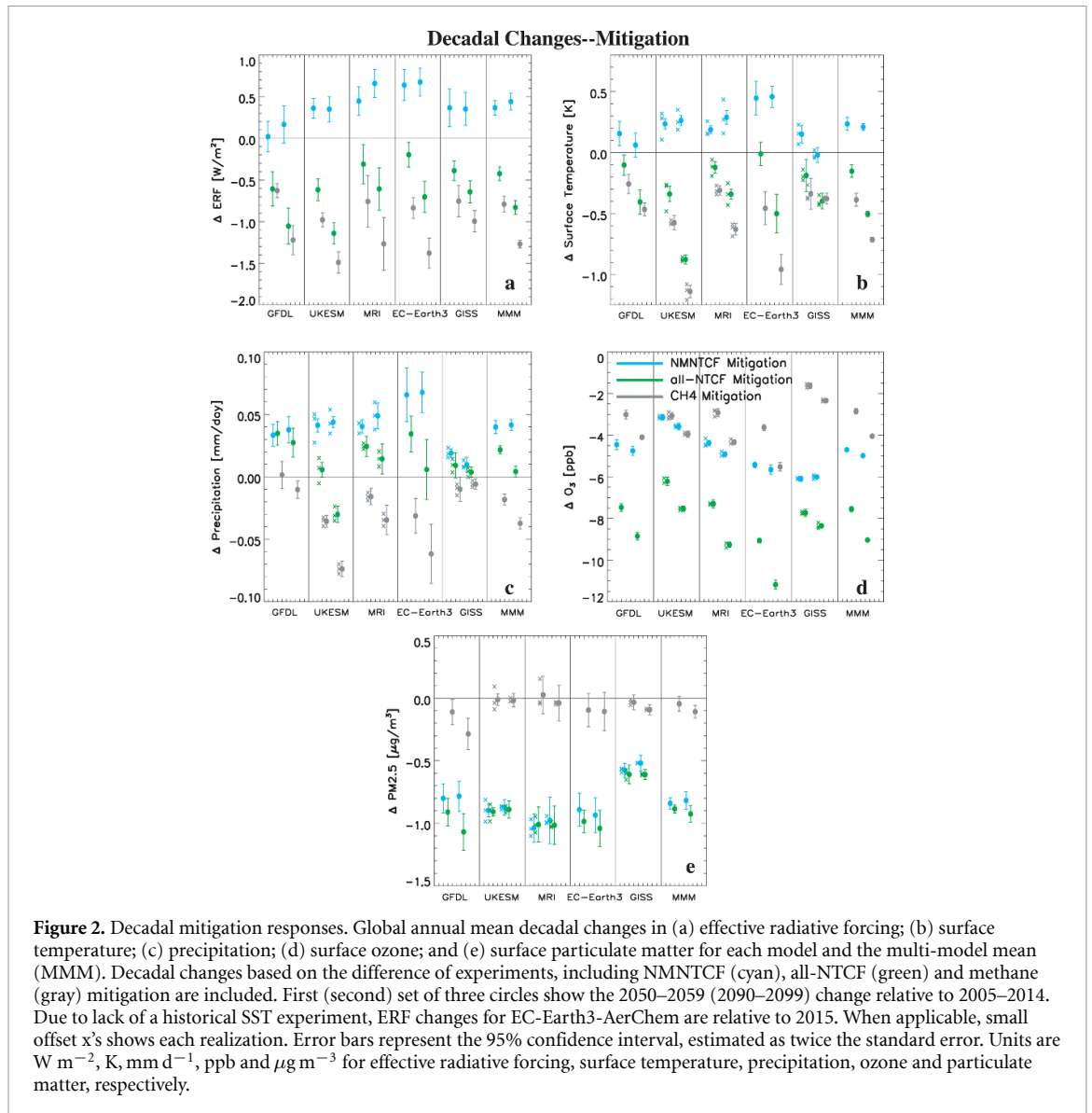


The five models used here span a relatively large range of effective equilibrium climate sensitivity, ranging from 2.6 K in GFDL-ESM4 to 5.3 K in UKESM1-0-LL; the corresponding transient climate response ranges from 1.6 K in both GFDL-ESM4 and GISS-E2-1-G to 2.8 K in UKESM1-0-LL (Meehl *et al* 2020). Furthermore, these models exhibit considerable ERF spread under NMNTCF, all-NTCF and methane mitigation (figure 2(a), table 1, supplementary figure 4 and supplement). However, an analysis comparing the surface temperature response sensitivity to ERF, and separately to a transient climate response (TCR)-like quantity (i.e. $\Delta T_s/ERF$ estimated from each of the mitigation signals) does not clearly indicate if ERF or TCR is more important in explaining the model spread in the surface temperature response under mitigation (supplementary table 2, supplementary figure 5 and supplement). We also note that three models account for shortwave absorption by methane, including UKESM1-0-LL, GFDL-ESM4 and EC-Earth3-AerChem. Two of these models, UKESM1-0-LL and EC-Earth3-AerChem have

the largest (negative) ERF due to methane mitigation (and the largest surface cooling). GFDL-ESM4, however, has the weakest ERF and surface cooling due to methane mitigation by mid-century, and the second weakest ERF and surface cooling due to methane mitigation by end-of-the-century. So there are other factors besides shortwave absorption by methane that account for the model spread in ERF (and surface temperature response) under methane mitigation.

3.2. Precipitation

In terms of global annual mean precipitation (figure 3 and supplementary figure 6), weak air quality control yields significant precipitation increases in all models, ranging from 0.016 to 0.145 mm d⁻¹ by mid-century and 0.059 to 0.305 mm d⁻¹ by end-of-the-century. The increase in precipitation is consistent with the increase in global mean temperature which accelerates the hydrological cycle (Held and Soden 2006). As with the surface temperature response, GFDL-ESM4 yields the weakest precipitation increase, and



UKESM1-0-LL yields the strongest precipitation increase. More generally, the correlation between the precipitation and surface temperature response across models is 0.93 for 2050–2059 and 0.94 for 2090–2099, both significant at the 99% confidence level (similar correlations apply for the other experiments, as well as with the mitigation signals). The corresponding MMM precipitation increase (figure 3(f)) is 0.065 ± 0.006 by mid-century and 0.158 ± 0.006 mm d^{-1} by end-of-the-century, or percent increases of 2.2% and 5.3%. Under strong non-methane air quality control, models show larger precipitation increases, consistent with the larger surface warming induced by decreases in aerosols and non-methane precursor gases. The precipitation increase ranges from 0.049 to 0.186 mm d^{-1} by mid-century and 0.087 to 0.349 mm d^{-1} by end-of-the-century, with GFDL-ESM4 and GISS-E2-1-G (UKESM1-0-LL) yielding the smallest (largest) increase (figure 3(f)). The corresponding MMM precipitation is 0.105 ± 0.007

and 0.200 ± 0.007 mm d^{-1} , respectively, or percent increases of 3.5% and 6.7%.

NMNTCF mitigation also yields a significant increase in global mean precipitation in all models (figure 2(c), table 1 and supplementary figure 7), with a MMM increase of 0.040 ± 0.005 mm d^{-1} by mid-century and 0.041 ± 0.004 mm d^{-1} by end-of-the-century, or percent increases of 1.3% and 1.4% respectively. This result is consistent with prior studies (Ramanathan *et al* 2001, Wilcox *et al* 2013, Samset *et al* 2016, Allen *et al* 2020) and with the increase in global mean temperature spinning up the hydrological cycle. Similarly, all-NTCF mitigation also yields a significant increase in global mean precipitation by mid-century (table 1), about half as large as that under NMNTCF mitigation, at 0.022 ± 0.003 mm d^{-1} (percent increase of 0.7%). Interestingly, this increase in precipitation occurs despite global cooling (recall, all-NTCF mitigation offsets the warming due to NMNTCF mitigation). This is likely related to the larger

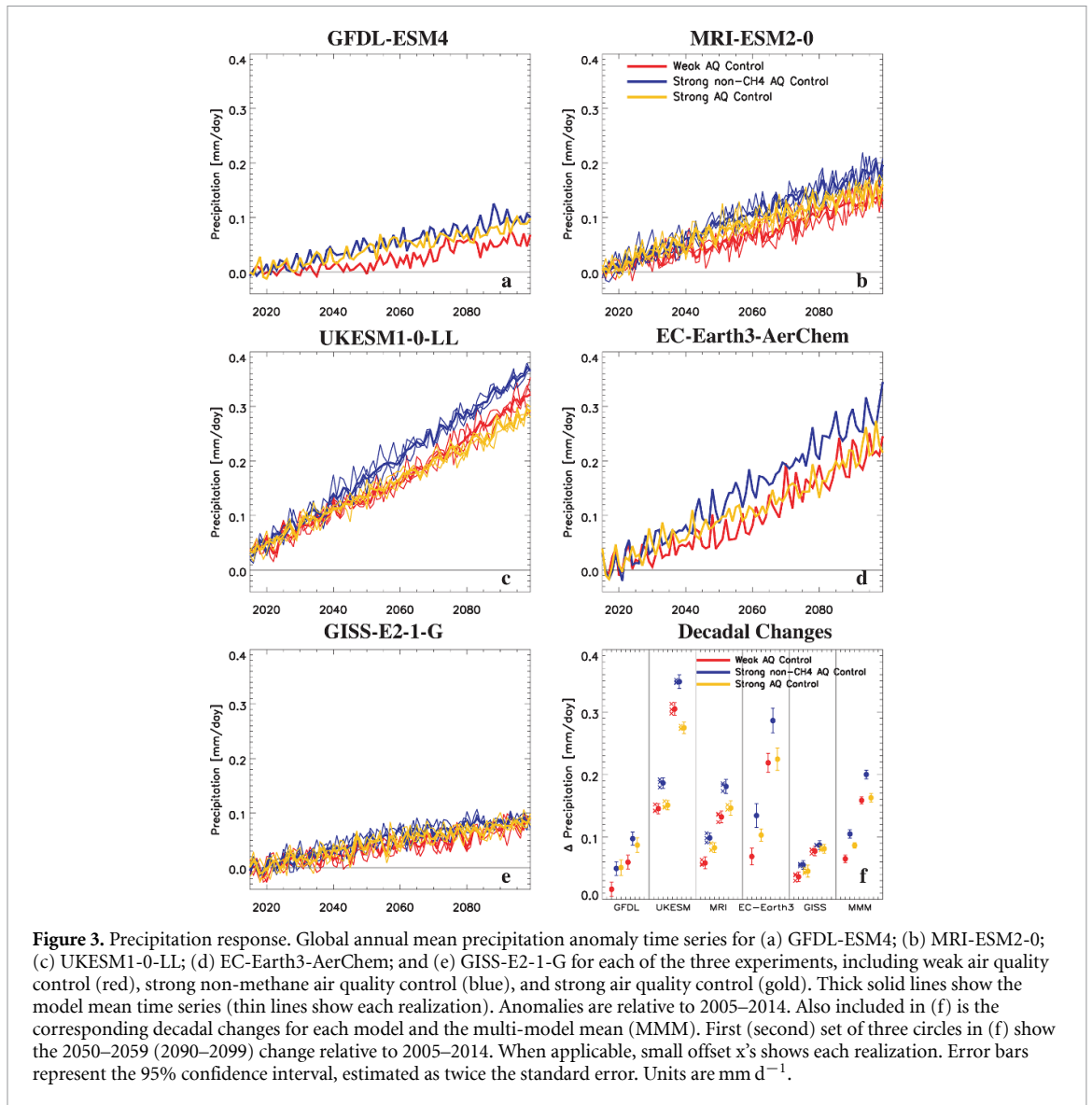


Figure 3. Precipitation response. Global annual mean precipitation anomaly time series for (a) GFDL-ESM4; (b) MRI-ESM2-0; (c) UKESM1-0-LL; (d) EC-Earth3-AerChem; and (e) GISS-E2-1-G for each of the three experiments, including weak air quality control (red), strong non-methane air quality control (blue), and strong air quality control (gold). Thick solid lines show the model mean time series (thin lines show each realization). Anomalies are relative to 2005–2014. Also included in (f) is the corresponding decadal changes for each model and the multi-model mean (MMM). First (second) set of three circles in (f) show the 2050–2059 (2090–2099) change relative to 2005–2014. When applicable, small offset x's shows each realization. Error bars represent the 95% confidence interval, estimated as twice the standard error. Units are mm d^{-1} .

apparent hydrological sensitivity (i.e. the change in precipitation per unit change in global surface temperature) of shortwave forcers like aerosols, relative to longwave forcers like methane (Liepert and Previdi 2009, Andrews *et al* 2010, Samset *et al* 2016, Liu *et al* 2018, Modak *et al* 2018), which implies the aerosol effect dominates—at least in the short-term. By end-of-the-century, with the weaker warming from aerosol and precursor gas emission reductions, but larger methane-induced cooling, all-NTCF mitigation yields a negligible MMM precipitation change of $0.004 \pm 0.004 \text{ mm d}^{-1}$, or a percent increase of 0.1%. As expected, methane mitigation (figure 2(c) and table 1) yields a significant decrease in global mean precipitation (except for GFDL-ESM4 by mid-century), with MMM decreases of -0.018 ± 0.004 and $-0.037 \pm 0.004 \text{ mm d}^{-1}$, or percent decreases of -0.6 and -1.3% , respectively. Finally, we note that a significant northward tropical rain belt shift also occurs under NMNTCF mitigation, most of which is cancelled out by

end-of-the-century under all-NTCF mitigation (supplement).

3.3. Air quality

We next analyze the impact of NTCF reductions on air quality, in terms of both surface O_3 and $\text{PM}_{2.5}$ (spatial maps are included in supplementary figures 8–11). Figure 4 shows the global mean O_3 anomaly time series and decadal changes for each of the three experiments. Weak air quality control results in a significant increase in O_3 in nearly all models, ranging from 0.68 to 1.90 ppb by mid-century and -0.37 to 1.81 ppb by end-of-the-century (figure 4(f)). Here, GFDL-ESM4 yield the largest increase, whereas GISS-E2-1-G yields the weakest increase (including the decrease by end-of-the-century). The corresponding MMM O_3 changes are 1.26 ± 0.10 and 0.71 ± 0.13 ppb, respectively, which equate to percent increases of 4.0% and 2.3%. The larger O_3 increase by mid-century is consistent with the increase in ozone precursors, including VOC, NO_x , CO and

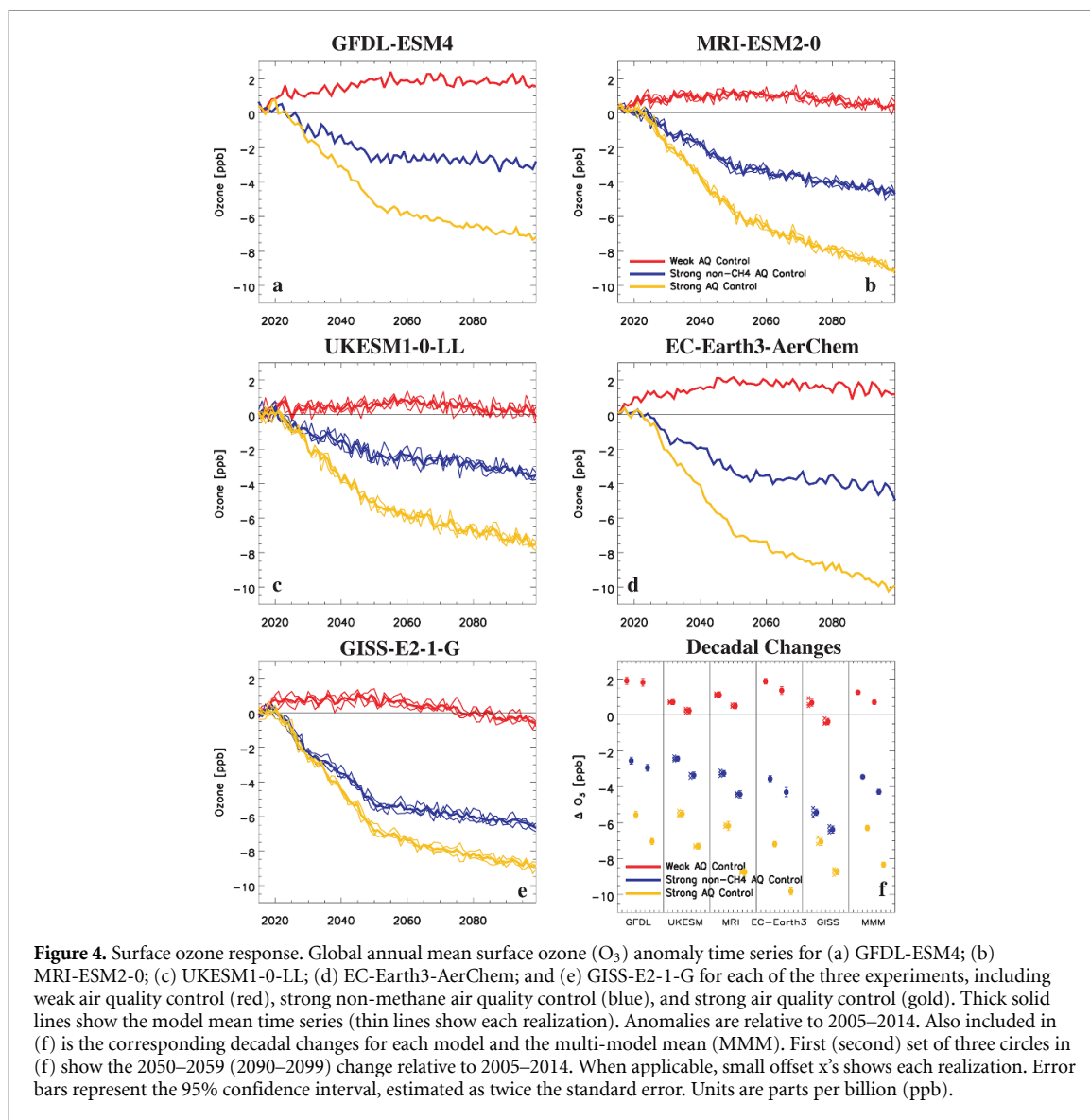


Figure 4. Surface ozone response. Global annual mean surface ozone (O_3) anomaly time series for (a) GFDL-ESM4; (b) MRI-ESM2-0; (c) UKESM1-0-LL; (d) EC-Earth3-AerChem; and (e) GISS-E2-1-G for each of the three experiments, including weak air quality control (red), strong non-methane air quality control (blue), and strong air quality control (gold). Thick solid lines show the model mean time series (thin lines show each realization). Anomalies are relative to 2005–2014. Also included in (f) is the corresponding decadal changes for each model and the multi-model mean (MMM). First (second) set of three circles in (f) show the 2050–2059 (2090–2099) change relative to 2005–2014. When applicable, small offset x's shows each realization. Error bars represent the 95% confidence interval, estimated as twice the standard error. Units are parts per billion (ppb).

CH_4 (supplementary figure 1). Under strong non-methane air quality control, significant O_3 decreases occur in all models, with a MMM decrease of -3.44 ± 0.10 ppb (-11.0%) by mid-century and -4.28 ± 0.14 ppb (-13.7%) by end-of-the-century (figure 4(f)). This is again consistent with reduced emissions of gaseous non-methane ozone precursors. In terms of NMNTCF mitigation, (figure 2(d) and table 1), O_3 decreases have MMM changes of -4.70 ± 0.07 ppb (-15.1%) by mid-century and -4.99 ± 0.06 ppb (-16.0%) by end-of-the-century. Unfortunately, as discussed above, this improvement in ozone-related air quality under NMNTCF mitigation comes at the price of additional increases in surface temperature (table 1 and figure 2(b)).

Relative to strong non-methane air quality control, strong air quality control yields even larger decreases in O_3 (figure 4(f)), with MMM changes of -6.30 ± 0.15 ppb (-20.2%) by mid-century and -8.33 ± 0.14 ppb (-26.7%) by end-of-the-century. This larger improvement in ozone-related air quality

is because methane, whose atmospheric concentration decreases by -34% under strong air quality control, is a precursor to tropospheric ozone (Prather *et al* 1994, Fiore *et al* 2012). In terms of all-NTCF mitigation (figure 2(d) and table 1), O_3 decreases occur in all models, with MMM decreases of -7.56 ± 0.13 ppb (-24.2%) by mid-century and -9.04 ± 0.07 ppb (-29.0%) by end-of-the-century. Under methane mitigation, a robust decrease in O_3 also occurs, with MMM decreases of -2.85 ± 0.13 ppb (-9.2%) by mid-century and -4.05 ± 0.05 ppb (-13.0%) by end-of-the-century. These methane-induced ozone decreases represent 38% and 45% of the all-NTCF induced ozone decreases by mid- and end-of-the-century. Thus, methane mitigation not only offsets warming due to reductions in NMNTCFs, but consistent with past studies (West *et al* 2007, Fiore *et al* 2008), causes additional improvements in ozone-related air quality.

Figure 5 shows global mean anomaly times series and decadal mean differences for surface particulate

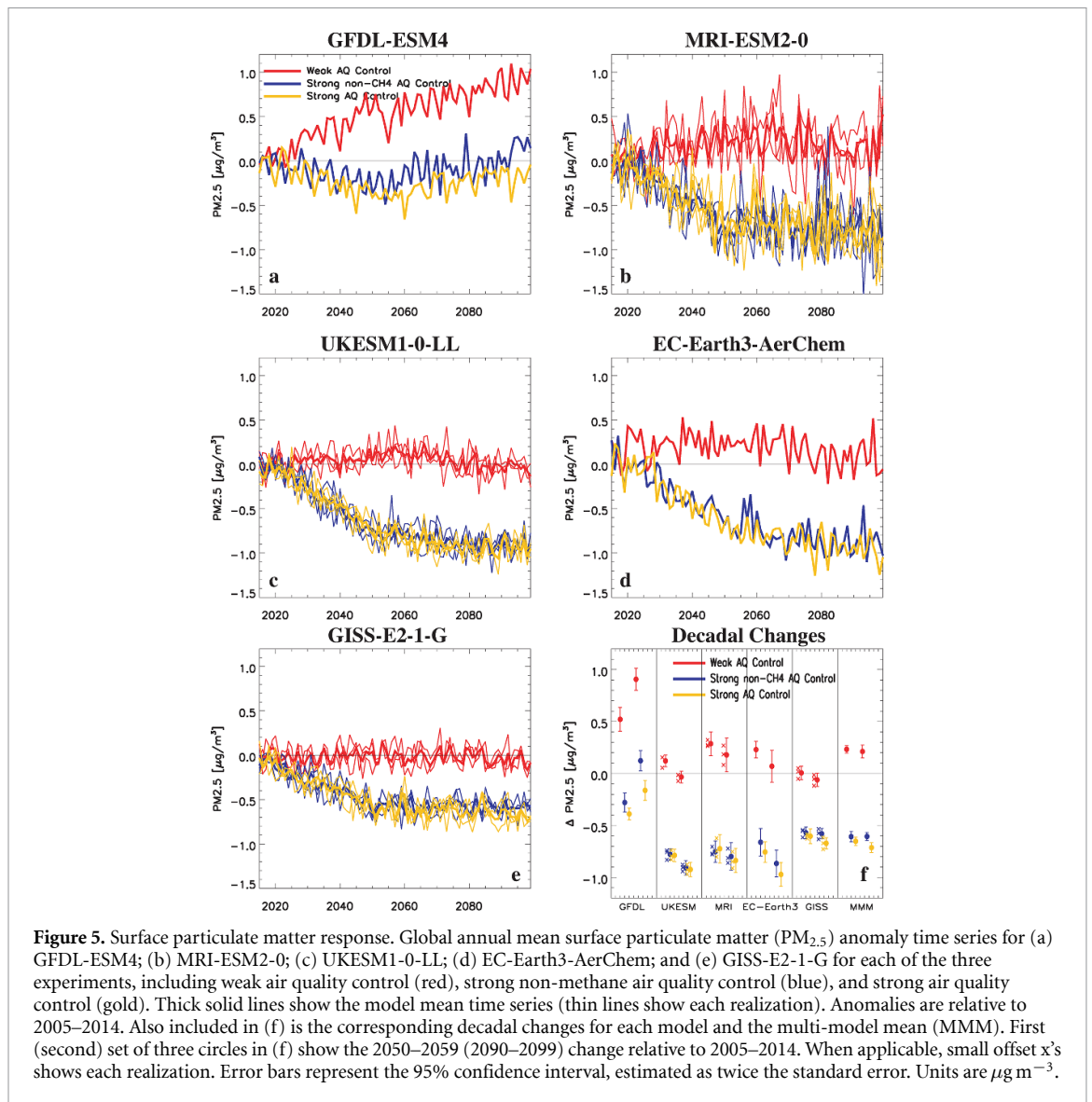


Figure 5. Surface particulate matter response. Global annual mean surface particulate matter ($PM_{2.5}$) anomaly time series for (a) GFDL-ESM4; (b) MRI-ESM2-0; (c) UKESM1-0-LL; (d) EC-Earth3-AerChem; and (e) GISS-E2-1-G for each of the three experiments, including weak air quality control (red), strong non-methane air quality control (blue), and strong air quality control (gold). Thick solid lines show the model mean time series (thin lines show each realization). Anomalies are relative to 2005–2014. Also included in (f) is the corresponding decadal changes for each model and the multi-model mean (MMM). First (second) set of three circles in (f) show the 2050–2059 (2090–2099) change relative to 2005–2014. When applicable, small offset x's shows each realization. Error bars represent the 95% confidence interval, estimated as twice the standard error. Units are $\mu\text{g m}^{-3}$.

matter, $PM_{2.5}$. Weak air quality control generally yields $PM_{2.5}$ increases, particularly by mid-century when most of the aerosol and gaseous precursors are increasing, ranging from 0.01 to $0.52 \mu\text{g m}^{-3}$ by mid-century and -0.06 to $0.91 \mu\text{g m}^{-3}$ by end-of-the-century. Similar to O_3 , GFDL-ESM4 yields the largest increase, whereas GISS-E2-1-G yields the weakest increase, including the 2100 decrease. The corresponding MMM changes (figure 5(f)) are 0.23 ± 0.04 and $0.21 \pm 0.06 \mu\text{g m}^{-3}$, which equate to $\sim 3.4\%$ increases. Consistent with the aerosol and gaseous precursor emission reductions, and (Allen *et al* 2020), strong non-methane air quality control yields significant $PM_{2.5}$ decreases by mid-century, ranging from -0.28 to $-0.78 \mu\text{g m}^{-3}$, with a MMM of $-0.61 \pm 0.05 \mu\text{g m}^{-3}$ (-9.0%). By end-of-the-century, models yield both significant decreasing and increasing $PM_{2.5}$, ranging from 0.12 (GFDL-ESM4) to -0.91 (UKESM1-0-LL) $\mu\text{g m}^{-3}$. The MMM, however, yields a significant decrease similar to that by mid-century (-9.0%). The $PM_{2.5}$

increase in GFDL-ESM4 by 2100—despite continued reductions in aerosol and gaseous precursors—is similar using archived $PM_{2.5}$ (not shown). This unexpected $PM_{2.5}$ increase results largely from increases in temperature-dependent sources of sea salt and biogenic secondary organic aerosols (Dunne *et al* 2020, Paulot *et al* 2020). Some of this also may be related to natural variability, or to the impact warming has on decreasing large scale precipitation, which has been shown to drive an increase in aerosol burden (Allen *et al* 2016, 2019, Park *et al* 2020). Nonetheless, NMNTCF mitigation (figure 2(e) and table 1) yields improvements in $PM_{2.5}$ -related air quality, including decreases ranging from -0.58 to $-1.04 \mu\text{g m}^{-3}$ by mid-century, and very similar decreases by end-of-the-century. The corresponding MMM $PM_{2.5}$ decreases are also similar in both time periods at -0.84 and $-0.82 \mu\text{g m}^{-3}$, respectively, or percent changes of -12.5% and -12.2% . We note that these $PM_{2.5}$ changes are likely too low—by a factor of $\sim 1/3$ —as our (approximated) $PM_{2.5}$ does

not include nitrate (NO₃) or ammonium (NH₄) aerosol (supplement, supplementary figures 12 and 13).

Relative to strong non-methane air quality control, strong air quality control yields similar PM_{2.5} decreases (figure 5(f)), with MMM changes of $-0.65 \pm 0.04 \mu\text{g m}^{-3}$ (−9.7%) by mid-century and $-0.71 \pm 0.05 \mu\text{g m}^{-3}$ (−10.6%) by end-of-the-century. Similarly, all-NTCF mitigation (figure 2(e) and table 1) yields similar PM_{2.5} decreases as NMNTCF mitigation, with MMM changes of -0.88 ± 0.03 (−13.2%) by mid-century and -0.93 ± 0.07 (−13.7%) by end-of-the-century. Although methane is a dominant sink of the hydroxyl radical (OH), the primary tropospheric oxidizing agent (Levy 1971), and changes in methane emissions will affect the lifetime of CH₄ and related gases (Prather 1994), including the formation of aerosols through oxidation of gaseous precursors (Shindell *et al* 2009, Karset *et al* 2018), we do not find additional decreases in PM_{2.5} under methane reductions. In fact, under methane mitigation, the change in PM_{2.5} is generally not significant in most models (GFDL-ESM4 being the exception for both time periods), ranging from -0.11 to $0.03 \mu\text{g m}^{-3}$ by mid-century and -0.29 to $-0.02 \mu\text{g m}^{-3}$ by end-of-the-century (table 1).

3.4. Regional responses

NTCF forcing, particularly the aerosol contribution, is spatially inhomogeneous (Shindell *et al* 2013), which can lead to regionally dependent responses. Prior studies have found aerosol reductions have relatively large warming and wetting impacts for much of Asia (including China) (Zheng *et al* 2020), and also impact climate extremes, with aerosols—as opposed to GHGs—having larger effects on temperature and precipitation extremes over China when normalized by global mean surface temperature change (Wang *et al* 2016). Consistent with this notion, we find that NMNTCF mitigation leads to larger decreases in ozone and in particular PM_{2.5}—and generally larger increases in surface temperature and precipitation—in regions with larger decreases in aerosols and precursor gas emissions, including several regions in Asia (supplement and supplementary figures 14–16). The inclusion of methane reductions, however, still offsets the enhanced warming due to NMNTCF mitigation in these regions, particularly by end-of-the-century. For example, the MMM change in surface temperature under all-NTCF mitigation in south Asia is -0.02 ± 0.11 K by mid-century and -0.32 ± 0.08 K by end-of-the-century (supplementary figure 14(b)). The corresponding changes in east Asia are -0.06 ± 0.13 and -0.27 ± 0.12 K (supplementary figure 15(b)); and -0.14 ± 0.11 K and -0.43 ± 0.10 K for southeast Asia (supplementary figure 16(b)). Inclusion of methane reductions also leads to larger decreases in O₃ in these regions (as with the global mean, similar PM_{2.5} decreases occur with

and without methane reductions). For example, in southeast Asia, O₃ decreases by -33.1% and -40.3% by mid- and end-of-the-century, as compared to -25.4% and -29.2% under NMNTCF mitigation (supplementary figure 16(f)).

As with the global mean precipitation results, all-NTCF mitigation continues to yield MMM precipitation increases in these regions, particularly by mid-century. That is, adding methane does not offset the wetting due to aerosol and precursor gas emission reductions—although by end-of-the-century, the MMM increase is relatively small and non-significant. For example, the MMM NMNTCF precipitation response for east Asia is 0.147 ± 0.04 and $0.146 \pm 0.06 \text{ mm d}^{-1}$ by mid- and end-of-the-century (supplementary figure 15(d)). Under all-NTCF mitigation, a significant precipitation increase remains by mid-century ($0.107 \pm 0.05 \text{ mm d}^{-1}$), whereas a weaker and non-significant increase exists by end-of-the-century ($0.076 \pm 0.080 \text{ mm d}^{-1}$). Similar results occur for south Asia, where the significant mid-century precipitation increase under NMNTCF mitigation of $0.190 \pm 0.07 \text{ mm d}^{-1}$ decreases only slightly under all-NTCF mitigation at $0.146 \pm 0.10 \text{ mm d}^{-1}$ (supplementary figure 14(d)). However, by end-of-the-century, the south Asia precipitation increase under NMNTCF mitigation ($0.150 \pm 0.04 \text{ mm d}^{-1}$) is negated under all-NTCF mitigation ($-0.001 \pm 0.07 \text{ mm d}^{-1}$). We also note that for both south Asia and east Asia, the largest precipitation increase under NMNTCF mitigation occurs during summertime (June–July–August; JJA), coincident with their wet (monsoon) season, and consistent with prior studies that show aerosol reductions drive wetting in several monsoon regions (Levy *et al* 2013, Westervelt *et al* 2017, 2018, Zhao *et al* 2018, Allen *et al* 2020). For both regions, the JJA precipitation increase is about two times larger than that based on the annual mean (not shown). Regardless, as with the annual mean, all-NTCF mitigation offsets this summertime precipitation increase by end-of-the-century for both south and east Asia. Thus, Asian regions in particular stand to benefit from NTCF mitigation, with relatively large improvements in air quality and negligible increases (if not decreases) in surface temperature and (by end-of-the-century) precipitation.

In the Arctic, warming in response to NMNTCF mitigation occurs in all models by mid-century, with relatively large MMM warming of 0.63 ± 0.10 K (supplementary figure 17). Weaker MMM warming exists by end-of-the-century at 0.42 ± 0.11 K, with two models (GFDL-ESM4 and GISS-E2-1-G) yielding non-significant warming. As with the global mean and Asian regions, however, including methane offsets most of the Arctic warming due to NMNTCF reductions, particularly by end-of-the-century. All-NTCF mitigation yields a negligible MMM temperature change of

-0.06 ± 0.14 K by mid-century, and significant cooling of -0.88 ± 0.10 K by end-of-the-century. NTCF mitigation (0.3% and -2.4% by mid- and end-of-the-century) also offsets Arctic wetting due to NMNTCF mitigation (2.7% and 3.1% by mid- and end-of-the-century) for both time periods. Significant improvements in Arctic air quality also occur under NTCF mitigation, with $\text{PM}_{2.5}$ decreasing by -19.7% and -22.1% by mid- and end-of-the-century; similarly, O_3 decreases by -24.8% and -31.0% , respectively. Interestingly, although not significant in all models, methane mitigation also yields a significant MMM decrease in Arctic $\text{PM}_{2.5}$ of $-0.04 \pm 0.01 \mu\text{g m}^{-3}$ by mid-century and $-0.11 \pm 0.01 \mu\text{g m}^{-3}$ by end-of-the-century (percent decreases of -2.7% and -6.7%).

4. Conclusions

As expected, NMNTCF mitigation yields significant improvements in air quality, in terms of both surface ozone and particulate matter, with some regions experiencing very large improvements (e.g. parts of Asia). However, reductions in aerosol and non-methane precursor gas emissions unmasks CO_2 warming, resulting in surface warming of 0.23 ± 0.05 K by mid-century and 0.21 ± 0.03 K by end-of-the-century, and corresponding precipitation increases of 0.040 ± 0.005 and $0.041 \pm 0.004 \text{ mm d}^{-1}$ (percent increases of 1.3% and 1.4%). These results are consistent with prior studies, including Allen *et al* (2020). Including methane reductions, however, more than offsets this enhanced warming due to NMNTCF mitigation during both the short- and long-term, with all-NTCF mitigation yielding global cooling of -0.15 ± 0.05 by mid-century and -0.50 ± 0.02 K by end-of-the-century. Although methane reductions also offset NMNTCF wetting by end-of-the-century, only about half of the wetting is offset by mid-century. The large Arctic warming (and wetting) under NMNTCF mitigation is also countered under all-NTCF mitigation—particularly by end-of-the-century. Furthermore, regions that experience the largest improvements in air quality under NMNTCF mitigation also tend to experience relatively large warming and wetting (e.g. Asian regions). All-NTCF mitigation again offsets much of this enhanced warming (but not the mid-century wetting), with significant cooling by end-of-the-century for several Asian regions under all-NTCF mitigation. Moreover, all-NTCF mitigation yields additional improvements in air quality as compared to NMNTCF mitigation, particularly enhanced surface ozone reductions (e.g. methane is responsible for 38% and 45% of the total global mean ozone decrease by mid-century and end-of-the-century, respectively). Our results therefore suggest that NTCF mitigation can improve air quality while simultaneously addressing climate change, and that methane

reductions can counter enhanced warming from aerosol and non-methane precursor gas emission reductions.

Data availability statement

The data that support the findings of this study are openly available at the following URL/DOI: <https://esgf-node.llnl.gov/search/cmip6>.

Acknowledgments



The data that support the findings of this study are openly available via the Earth System Grid Federation (ESGF) at <https://esgf-node.llnl.gov/search/cmip6/>. S Shim was supported by the Korea Meteorological Administration Research and Development Program ‘Development and Assessment of IPCC AR6 Climate Change Scenario’, Grant Agreement No. KMA2018-00321. M Deushi and N Oshima were supported by the Japan Society for the Promotion of Science (Grant Nos. JP18H03363, JP18H05292, JP19K12312 and JP20K04070), the Environment Research and Technology Development Fund (JPMEERF20172003, JPMEERF20202003, and JPMEERF20205001) of the Environmental Restoration and Conservation Agency of Japan, the Arctic Challenge for Sustainability II (ArCS II), Program Grant Number JPMXD1420318865, and a grant for the Global Environmental Research Coordination System from the Ministry of the Environment, Japan P Le Sager and T van Noije acknowledge the EU CRESCENDO project. G A Folberth and F M O’Connor were also supported by the Met Office Hadley Centre Climate Programme funded by BEIS and Defra (GA01101). S Turnock would like to acknowledge the UK-China Research and Innovation Partnership Fund through the Met Office Climate Science for Service Partnership (CSSP) China as part of the Newton Fund L Horowitz, V Naik, L Sentman, and J John thank the GFDL model development team and the leadership of NOAA/GFDL for their efforts and support in developing ESM4 as well as the GFDL modeling systems group and data portal team for technical support to make data available at ESGF. P Le Sager, T van Noije, G A Folberth and F M O’Connor acknowledge the EU Horizon 2020 Research Programme CRESCENDO project, Grant Agreement Number 641816.

ORCID iDs

Robert J Allen  <https://orcid.org/0000-0003-1616-9719>

Naga Oshima  <https://orcid.org/0000-0002-8451-2411>

Makoto Deushi  <https://orcid.org/0000-0002-0373-3918>

Shinichiro Fujimori  <https://orcid.org/0000-0001-7897-1796>
 William J Collins  <https://orcid.org/0000-0002-7419-0850>

References

- Allen R J 2015 A 21st century northward tropical precipitation shift caused by future anthropogenic aerosol reductions *J. Geophys. Res.: Atmos.* **120** 9087–102
- Allen R J et al 2020 Climate and air quality impacts due to mitigation of non-methane near-term climate forcers *Atmos. Chem. Phys.* **20** 9641–63
- Allen R J and Ajoku O 2016 Future aerosol reduction and widening of the northern tropical belt *J. Geophys. Res.* **121** 6765–86
- Allen R J, Evan A T and Booth B B B 2015 Interhemispheric aerosol radiative forcing and tropical precipitation shifts during the late twentieth century *J. Clim.* **28** 8219–46
- Allen R J, Hassan T, Randles C A and Su H 2019 Enhanced land-sea warming contrast elevates aerosol pollution in a warmer world *Nat. Clim. Change* **9** 300–5
- Allen R J, Landuyt W and Rumbold S T 2016 An increase in aerosol burden and radiative effects in a warmer world *Nat. Clim. Change* **6** 269–74
- Andreae M O, Jones C D and Cox P M 2005 Strong present-day aerosol cooling implies a hot future *Nature* **435** 1187–90
- Andrews T, Forster P M, Boucher O, Bellouin N and Jones A 2010 Precipitation, radiative forcing and global temperature change *Geophys. Res. Lett.* **37** L14701
- Archibald A T et al 2020 Description and evaluation of the UKCA stratosphere–troposphere chemistry scheme (StratTrop v1.0) implemented in UKESM1 *Geosci. Model Dev.* **13** 1223–66
- Arneth A, Unger N, Kulmala M and Andreae M O 2009 Clean the air, heat the planet? *Science* **326** 672–3
- Bauer S E, Tsigaridis K, Faluvegi G, Kelley M, Lo K K, Miller R L, Nazarenko L, Schmidt G A and Wu J 2020 Historical (1850–2014) aerosol evolution and role on climate forcing using the GISS ModelE2.1 contribution to CMIP6 *J. Adv. Model. Earth Syst.* **12** e2019MS001978
- Brasseur G P and Roeckner E 2005 Impact of improved air quality on the future evolution of climate *Geophys. Res. Lett.* **32** L23704
- Butt E W et al 2017 Global and regional trends in particulate air pollution and attributable health burden over the past 50 years *Environ. Res. Lett.* **12** 104017
- Clarke L et al 2014 Assessing transformation pathways *Climate Change 2014: Mitigation of Climate Change. Contribution of Working Group III to the Fifth Assessment Report of the Intergovernmental Panel on Climate Change Technical Report* ed O Edenhofer (Cambridge: Cambridge University Press)
- Cohen A J et al 2017 Estimates and 25-year trends of the global burden of disease attributable to ambient air pollution: an analysis of data from the Global Burden of Diseases Study 2015 *Lancet* **389** 1907–18
- Collins W D et al 2006 Radiative forcing by well-mixed greenhouse gases: estimates from climate models in the Intergovernmental Panel on Climate Change (IPCC) Fourth Assessment Report (AR4) *J. Geophys. Res.: Atmos.* **111** D14317
- Collins W J et al 2017 AerChemMIP: quantifying the effects of chemistry and aerosols in CMIP6 *Geosci. Model Dev.* **10** 585–607
- Dunne J P et al 2020 The GFDL Earth System Model version 4.1 (GFDL-ESM 4.1): overall coupled model description and simulation characteristics *J. Adv. Model. Earth Syst.* **12** e2019MS002015
- Etmann M, Myhre G, Highwood E J and Shine K P 2016 Radiative forcing of carbon dioxide, methane and nitrous oxide: a significant revision of the methane radiative forcing *Geophys. Res. Lett.* **43** 12614–23
- Eyring V, Bony S, Meehl G A, Senior C A, Stevens B, Stouffer R J and Taylor K E 2016 Overview of the coupled model intercomparison project phase 6 (CMIP6) experimental design and organization *Geosci. Model Dev.* **9** 1937–58
- Fiore A M et al 2012 Global air quality and climate *Chem. Soc. Rev.* **41** 6663–83
- Fiore A M, West J J, Horowitz L W, Naik V and Schwarzkopf M D 2008 Characterizing the tropospheric ozone response to methane emission controls and the benefits to climate and air quality *J. Geophys. Res.: Atmos.* **113** D08307
- Forster P M, Richardson T, Maycock A C, Smith C J, Samset B H, Myhre G, Andrews T, Pincus R and Schulz M 2016 Recommendations for diagnosing effective radiative forcing from climate models for CMIP6 *J. Geophys. Res.: Atmos.* **121** 12460–75
- Fujimori S, Hasegawa T, Masui T, Takahashi K, Herran D S, Dai H, Hijioka Y and Kainuma M 2017 SSP3: AIM implementation of shared socioeconomic pathways *Glob. Environ. Change* **42** 268–83
- Gidden M J et al 2019 Global emissions pathways under different socioeconomic scenarios for use in CMIP6: a dataset of harmonized emissions trajectories through the end of the century *Geosci. Model Dev.* **12** 1443–75
- Haines A, Amann M, Borgford-Parnell N, Leonard S, Kuylenstierna J and Shindell D 2017 Short-lived climate pollutant mitigation and the sustainable development goals *Nat. Clim. Change* **7** 863–9
- Held I M and Soden B J 2006 Robust responses of the hydrological cycle to global warming *J. Clim.* **19** 5686–99
- Hienola A, Partanen A-I, Pietikäinen J-P, O'Donnell D, Korhonen H, Matthews H D and Laaksonen A 2018 The impact of aerosol emissions on the 1.5 °C pathways *Environ. Res. Lett.* **13** 044011
- Horowitz L W et al 2020 The GFDL global atmospheric chemistry-climate model AM4.1: model description and simulation characteristics *J. Adv. Model. Earth Syst.* **12** e2019MS002032
- Horowitz L W, Naik V, Sentman L T, Paulot F, Blanton C, McHugh C, Radhakrishnan A, Rand K, Ginoux P and Paynter D J 2018 NOAA-GFDL GFDL-ESM4 model output prepared for CMIP6 AerChemMIP Version 201807011. *Earth System Grid Federation* (available at: <https://doi.org/10.22033/ESGF/CMIP6.1404>)
- IPCC 2018 Summary for policymakers. Global Warming of 1.5 °C. An IPCC special report on the impacts of global warming of 1.5 °C above pre-industrial levels and related global greenhouse gas emission pathways, in the context of strengthening the global response to the threat of climate change, sustainable development and efforts to eradicate poverty *Technical Report* ed V Masson-Delmotte et al (Geneva: World Meteorological Organization) p 32
- John J G et al 2018 NOAA-GFDL GFDL-ESM4 model output prepared for CMIP6 ScenarioMIP Version 201807011. *Earth System Grid Federation* (available at: <https://doi.org/10.22033/ESGF/CMIP6.1414>)
- Jones A, Haywood J M and Jones C D 2018 Can reducing black carbon and methane below RCP2.6 levels keep global warming below 1.5 °C? *Atmos. Sci. Lett.* **19** e821
- Karset I H H et al 2018 Strong impacts on aerosol indirect effects from historical oxidant changes *Atmos. Chem. Phys.* **18** 7669–90
- Kloster S, Dentener F, Feichter J, Raes F, Lohmann U, Roeckner E and Fischer-Bruns I 2010 A GCM study of future climate response to aerosol pollution reductions *Clim. Dyn.* **34** 1177–94
- Lelieveld J 2017 Clean air in the anthropocene *Faraday Discuss.* **200** 693–703

- Lelieveld J, Klingmüller K, Pozzer A, Burnett R T, Haines A and Ramanathan V 2019 Effects of fossil fuel and total anthropogenic emission removal on public health and climate *Proc. Natl Acad. Sci.* **116** 7192–7
- Levy H 1971 Normal atmosphere: large radical and formaldehyde concentrations predicted *Science* **173** 141–3
- Levy H, Horowitz L W, Schwarzkopf M D, Ming Y, Golaz J-C, Naik V and Ramaswamy V 2013 The roles of aerosol direct and indirect effects in past and future climate change *J. Geophys. Res.: Atmos.* **118** 4521–32
- Liepert B G and Previdi M 2009 Do models and observations disagree on the rainfall response to global warming? *J. Clim.* **22** 3156–66
- Liu L et al 2018 A PDRMIP multimodel study on the impacts of regional aerosol forcings on global and regional precipitation *J. Clim.* **31** 4429–47
- Matthews H D and Zickfeld K 2012 Climate response to zeroed emissions of greenhouse gases and aerosols *Nat. Clim. Change* **2** 338–41
- Meehl G A, Senior C A, Eyring V, Flato G, Lamarque J-F, Stouffer R J, Taylor K E and Schlund M 2020 Context for interpreting equilibrium climate sensitivity and transient climate response from the CMIP6 Earth system models *Sci. Adv.* **6** eaba1981
- Modak A, Bala G, Caldeira K and Cao L 2018 Does shortwave absorption by methane influence its effectiveness? *Clim. Dyn.* **51** 3653–72
- Mulcahy J P et al 2020 Description and evaluation of aerosol in UKESM1 and HadGEM3-GC3.1 CMIP6 historical simulations *Geosci. Model Dev. Discuss.* **2020** 1–59
- Myhre G et al 2013 Anthropogenic and natural radiative forcing *Climate Change 2013: The Physical Science Basis. Contribution of Working Group I to the Fifth Assessment Report of the Intergovernmental Panel on Climate Change Technical Report* ed T F Stocker et al (Cambridge: Cambridge University Press)
- O'Neill B C et al 2016 The scenario model intercomparison project (ScenarioMIP) for CMIP6 *Geosci. Model Dev.* **9** 3461–82
- O'Neill B C, Kriegler E, Riahi K, Ebi K L, Hallegatte S, Carter T R, Mathur R and van Vuuren D P 2014 A new scenario framework for climate change research: the concept of shared socioeconomic pathways *Clim. Change* **122** 387–400
- Oshima N, Yukimoto S, Deushi M, Koshiro T, Kawai H, Tanaka T Y and Yoshida K 2020 Global and Arctic effective radiative forcing of anthropogenic gases and aerosols in MRI-ESM2.0 *Prog. Earth Planet. Sci.* **7** 38
- Park S, Allen R J and Lim C H 2020 A likely increase in fine particulate matter and premature mortality under future climate change *Air Qual. Atmos. Health* **13** 143–51
- Paulot F, Paynter D, Winton M, Ginoux P, Zhao M and Horowitz L W 2020 Revisiting the impact of sea salt on climate sensitivity *Geophys. Res. Lett.* **47** e2019GL085601
- Pincus R, Forster P M and Stevens B 2016 The Radiative Forcing Model Intercomparison Project (RFMIP): experimental protocol for CMIP6 *Geosci. Model Dev.* **9** 3447–60
- Prather M 1994 Lifetimes and eigenstates in atmospheric chemistry *Geophys. Res. Lett.* **21** 801–4
- Prather M, Derwent R, Ehhalt D, Fraser P, Sanhueza E and Zhou X 1994 Chapter 2: other tracer gases and atmospheric chemistry *Climate Change 1994, Intergovernmental Panel on Climate Change Technical Report* ed J T Houghton, Y Ding, D J Griggs, M Noguer, P J van der Linden, X Dai, K Maskell and C A Johnson (Cambridge: Cambridge University Press) pp 73–126
- Raes F and Seinfeld J H 2009 New directions: climate change and air pollution abatement: a bumpy road *Atmos. Environ.* **43** 5132–3
- Ramanathan V et al 2001 Indian Ocean Experiment: an integrated analysis of the climate forcing and effects of the great Indo-Asian haze *J. Geophys. Res.* **106** 28,371–28,398
- Ramanathan V and Feng Y 2008 On avoiding dangerous anthropogenic interference with the climate system: formidable challenges ahead *Proc. Natl Acad. Sci.* **105** 14245–50
- Rao S et al 2017 Future air pollution in the shared socio-economic pathways *Glob. Environ. Change* **42** 346–58
- Richardson T B et al 2018 Drivers of precipitation change: an energetic understanding *J. Clim.* **31** 9641–57
- Rotstajn L D, Collier M A, Chrastansky A, Jeffrey S J and Luo J J 2013 Projected effects of declining aerosol in RCP4.5: unmasking global warming? *Atmos. Chem. Phys.* **13** 10883–905
- Rotstajn L D, Collier M A and Luo J-J 2015a Effects of declining aerosols on projections of zonally averaged tropical precipitation *Environ. Res. Lett.* **10** 044018
- Rotstajn L D, Collier M A, Shindell D T and Boucher O 2015b Why does aerosol forcing control historical global-mean surface temperature change in CMIP5 models? *J. Clim.* **28** 6608–25
- Salzmann M 2016 Global warming without global mean precipitation increase? *Sci. Adv.* **2** e1501572
- Samset B H et al 2016 Fast and slow precipitation responses to individual climate forcings: a PDRMIP multimodel study *Geophys. Res. Lett.* **43** 2782–91
- Samset B H, Sand M, Smith C J, Bauer S E, Forster P M, Fuglestedt J S, Osprey S and Schluessner C-F 2018 Climate impacts from a removal of anthropogenic aerosol emissions *Geophys. Res. Lett.* **45** 1020–9
- Scannell C et al 2019 The influence of remote aerosol forcing from industrialized economies on the future evolution of east and west African rainfall *J. Clim.* **32** 8335–54
- Sellar A A et al 2019 UKESM1: description and evaluation of the U.K. Earth System Model *J. Adv. Model. Earth Syst.* **11** 4513–58
- Shindell D T et al 2012 Simultaneously mitigating near-term climate change and improving human health and food security *Science* **335** 183–9
- Shindell D T et al 2013 Radiative forcing in the ACCMIP historical and future climate simulations *Atmos. Chem. Phys.* **13** 2939–74
- Shindell D T et al 2017 A climate policy pathway for near- and long-term benefits *Science* **356** 493–4
- Shindell D T, Faluvegi G, Koch D M, Schmidt G A, Unger N and Bauer S E 2009 Improved attribution of climate forcing to emissions *Science* **326** 716–18
- Shindell D T and Smith C J 2019 Climate and air-quality benefits of a realistic phase-out of fossil fuels *Nature* **573** 408–11
- Silva R A et al 2017 Future global mortality from changes in air pollution attributable to climate change *Nat. Clim. Change* **7** 647–51
- Smith S J and Mizrahi A 2013 Near-term climate mitigation by short-lived forcings *Proc. Natl Acad. Sci.* **35** 14202–6
- Stohl A et al 2015 Evaluating the climate and air quality impacts of short-lived pollutants *Atmos. Chem. Phys.* **15** 10529–66
- Turnock S T et al 2020 Historical and future changes in air pollutants from CMIP6 models *Atmos. Chem. Phys. Discuss.* **2020** 1–40
- Turnock S T, Smith S and O'Connor F M 2019 The impact of climate mitigation measures on near term climate forcings *Environ. Res. Lett.* **14** 104013
- UNEP 2011 Near-term climate protection and clean air benefits: actions for controlling short-lived climate forcings *Technical Report* (Nairobi: United Nations Environment Programme) p 78
- van Noije T P C et al 2020 EC-Earth3-AerChem, a global climate model with interactive aerosols and atmospheric chemistry participating in CMIP6 *Geosci. Model Dev.* accepted
- van Noije T P C, Le Sager P, Segers A J, van Velthoven P F J, Krol M C, Hazeleger W, Williams A G and Chambers S D 2014 Simulation of tropospheric chemistry and aerosols with the climate model EC-Earth *Geosci. Model Dev.* **7** 2435–75

- van Vuuren D P *et al* 2014 A new scenario framework for climate change research: scenario matrix architecture *Clim. Change* **122** 373–86
- Wang Z, Lin L, Yang M and Xu Y 2016 The effect of future reduction in aerosol emissions on climate extremes in China *Clim. Dyn.* **47** 2885–99
- West J J, Fiore A M, Naik V, Horowitz L W, Schwarzkopf M D and Mauzerall D L 2007 Ozone air quality and radiative forcing consequences of changes in ozone precursor emissions *Geophys. Res. Lett.* **34** L06806
- Westervelt D M *et al* 2018 Connecting regional aerosol emissions reductions to local and remote precipitation responses *Atmos. Chem. Phys.* **18** 12461–75
- Westervelt D M, Conley A J, Fiore A M, Lamarque J-F, Shindell D T, Previdi M, Faluvegi G, Correa G and Horowitz L W 2017 Multimodel precipitation responses to removal of U.S. sulfur dioxide emissions *J. Geophys. Res.: Atmos.* **122** 5024–38
- Westervelt D M, Horowitz L W, Naik V, Golaz J-C and Mauzerall D L 2015 Radiative forcing and climate response to projected 21st century aerosol decreases *Atmos. Chem. Phys.* **15** 12681–703
- WHO 2016 Ambient air pollution: a global assessment of exposure and burden of disease *Technical Report* (Geneva: World Health Organization)
- Wilcox L J, Highwood E J and Dunstone N J 2013 The influence of anthropogenic aerosol on multi-decadal variations of historical global climate *Environ. Res. Lett.* **8** 024033
- Wu P, Christidis N and Stott P 2013 Anthropogenic impact on Earth's hydrological cycle *Nat. Clim. Change* **3** 807 E
- Yukimoto S *et al* 2019 The meteorological research institute earth system model version 2.0, MRI-ESM2.0: description and basic evaluation of the physical component *J. Meteor. Soc. Japan* **97** 931–65
- Zanis P *et al* 2020 Fast responses on pre-industrial climate from present-day aerosols in a CMIP6 multi-model study *Atmos. Chem. Phys. Discuss.* **2020** 1–32
- Zhao A D, Stevenson D S and Bollasina M A 2018 The role of anthropogenic aerosols in future precipitation extremes over the Asian Monsoon region *Clim. Dyn.* **52** 6257–78
- Zheng Y, Zhang Q, Tong D, Davis S J and Caldeira K 2020 Climate effects of China's efforts to improve its air quality *Environ. Res. Lett.* **15** 104052